Chemical Vapor Deposition

Vol. 20 (2014) September

Chemical Vapor Deposition
Prof. Michael L. Hitchman
Dept. of Pure and Applied Chemistry
University of Strathclyde
295 Cathedral Street
Glasgow G1 1XL (UK)
Tel.: + 44 (0) 141 587 7595
e-mail: m.l.hitchman@strath.ac.uk

Chemical Vapor Deposition
Advanced Materials
WILEY-VCH
Boschstrasse 12
D-69469 Weinheim (Germany)
Tel.: + 49 (0) 6201 606 235
Fax: + 49 (0) 6201 606 500
e-mail: advmat@wiley-vch.de

Contents http://www.cvd-journal.de

Cover image from M. M. Shawrav, H. D. Wanzenboeck, and co-workers (*Chem. Vap. Deposition* **2014**, *20*, 251)

The cover image illustrates the use of focused-electron-beam-induced CVD to directly write nanostructures with nanometer resolution. The Au-Fe nanoalloys produced have potential applications in nanoelectronics.

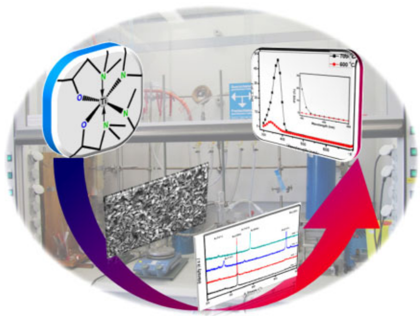

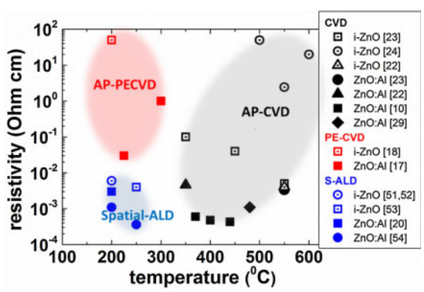
resistivity (Ohm cm)
10^2
10^1
10^0
10^{-1}
10^{-2}
10^{-3}
10^{-4}
100
200
300
400
500
600
temperature (^{o}C)
AP-PECVD
AP-CVD
Spatial-ALD
CVD
i-ZnO [23]
i-ZnO [24]
i-ZnO [22]
ZnO:Al [23]
ZnO:Al [22]
ZnO:Al [10]
ZnO:Al [29]
PE-CVD
i-ZnO [18]
ZnO:Al [17]
S-ALD
i-ZnO [51,52]
i-ZnO [53]
ZnO:Al [20]
ZnO:Al [54]

Full Paper: Focused electron beam-induced deposition (FEBID) is used as a direct-write approach for the fabrication of Fe-based nanostructures on Si(100), starting from $Fe(CO)_5$. FEBID uses an electron beam to locally induce a CVD process. A systematic variation of FEBID parameters is performed to study their influence on the geometry and composition of the deposit. Based on the results, specific deposition conditions are suggested for nanomagnetic applications and the fabrication of large structures.

M. Gavagnin, H. D. Wanzenboeck,* M. M. Shawrav, D. Belic, S. Wachter, S. Waid, M. Stoeger–Pollach, E. Bertagnolli

Chem. Vap. Deposition **2014**, *20*, 243 ... 250

Focused Electron Beam-Induced CVD of Iron: a Practical Guide for Direct Writing

---

Full Paper: Focused electron beam-induced deposition is utilized to co-deposit gold and iron structures using dimethyl-gold(III)-trifluoroacetylacetonate and iron pentacarbonyl metal-organic precursors. The deposition rate and chemical composition of these direct-write Au-Fe nanoalloys can be controlled by varying the working pressures.

M. M. Shawrav, D. Belić, M. Gavagnin, S. Wachter, M. Schinnerl, H. D. Wanzenboeck,* E. Bertagnolli

Chem. Vap. Deposition **2014**, *20*, 251 ... 257

Electron Beam-Induced CVD of Nanoalloys for Nanoelectronics

Full Paper: Thin films and nanoparticles of PtO_x ($2.5 < x < 2.7$) are deposited by plasma-assisted ALD in a temperature window from room temperature to 300 °C by controlling the O_2 plasma and $(MeCp)PtMe_3$ exposure. With increasing substrate temperature, the thermal stability of PtO_x is found to decrease and the reducing activity of the precursor ligands is found to increase. The material properties of the PtO_x films are studied and it is shown that a film conformality of 90% can be achieved in trenches with an aspect ratio of 9.

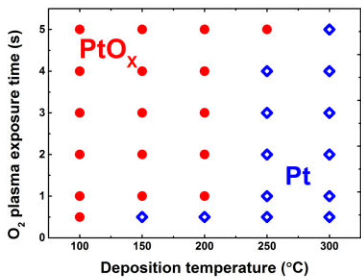

I. J. M. Erkens, M. A. Verheijen, H. C. M. Knoops, T. F. Landaluce, F. Roozeboom, W. M. M. Kessels*

Chem. Vap. Deposition **2014**, *20*, 258 ... 268

Plasma-Assisted Atomic Layer Deposition of PtO_x from $(MeCp)PtMe_3$ and O_2 Plasma

---

Full Paper: Thin films of Ca-doped $LaPO_4$ are produced using ALD with $La(thd)_3$, $(CH_3)_3PO_4$, H_2O, and O_3 as precursors. The films are studied using X-ray based techniques and TEM. The requirement of a mixed O_3/H_2O precursor for the growth of the phosphate is studied in detail using QCM.

H. H. Sønsteby, E. Østreng, H. Fjellvåg, O. Nilsen*

Chem. Vap. Deposition **2014**, *20*, 269 ... 273

Atomic Layer Deposition of $LaPO_4$ and $Ca:LaPO_4$

Full Paper: The luminescence properties of amorphous europium titanium oxide thin films grown by atomic layer deposition are investigated as a function of Eu_2O_3 and TiO_2 layer thicknesses, varying from a homogeneous mixture to 2.9 nm repeating layer structures. Samples ranging from homogeneous to 0.8 nm repeating layers are optically similar while the luminescence intensity decreases for thicker layers.

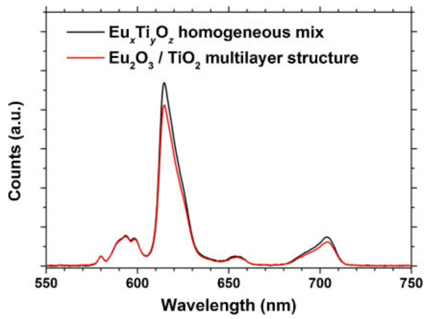

P.-A. Hansen, H. Fjellvåg, T. G. Finstad, O. Nilsen*

Chem. Vap. Deposition **2014**, *20*, 274 ... 281

Luminescent Properties of Multilayered Eu_2O_3 and TiO_2 Grown by Atomic Layer Deposition

---

Full Paper: The resistive switching of TiO_x/Al_2O_3 bilayers integrated in μ-crossbar devices is investigated for future ReRAM. The bilayer stack is realized in consecutive atomic layer depositions (ALD) at 300 °C. Amorphous Al_2O_3 films exhibit a dielectric permittivity of 8.0 and disruptive field strength of 7 MV cm^{-1}, whereas the oxygen-deficient TiO_x is semiconducting. The bipolar-type resistive switching characteristics of $TiN/TiO_x/Al_2O_3/Pt$ cells show a strong dependence on both oxide layer thicknesses.

H. Zhang, N. Aslam, M. Reiners, R. Waser, S. Hoffmann-Eifert*

Chem. Vap. Deposition **2014**, *20*, 282 ... 290

Atomic Layer Deposition of TiO_x/Al_2O_3 Bilayer Structures for Resistive Switching Memory Applications

---

Full Paper: Nanoscopic VO_x coatings are produced by atomic layer deposition for resistive random access memory devices. The devices show bipolar switching behavior with resistance ratio $R_{OFF}/R_{ON}>10^3$ whereas, at higher electroforming voltage (4 - 5 V), threshold switching behavior is observed.

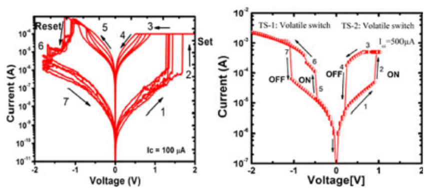

T. Singh, S. Wang, N. Aslam, H. Zhang, S. Hoffmann-Eifert, S. Mathur*

Chem. Vap. Deposition **2014**, *20*, 291 ... 297

Atomic Layer Deposition of Transparent VO_x Thin Films for Resistive Switching Applications

---

Review: A thermodynamic analysis is performed to comment on the stability of vanadium oxide structures based on the calculated formation energies. The structure-related properties of the identified stable and metastable compounds are discussed, with an emphasis on the reported functional applications. Finally, the established gas-phase chemical deposition processes for the growth of vanadium oxide compounds are reviewed, referring to the type of precursors used.

N. Bahlawane,* D. Lenoble

Chem. Vap. Deposition **2014**, *20*, 299 ... 311

Vanadium Oxide Compounds: Structure, Properties, and Growth from the Gas Phase

Full Paper: A two-step synthetic strategy for the synthesis of Fe_2O_3/CuO composites is presented. The approach consists of the growth of ε-Fe_2O_3 by CVD, followed by copper sputtering and annealing in air. A multi-technique characterization showed ε-Fe_2O_3 nanorod arrays possessing an intimate contact with nanometer-sized CuO particles, the loading and dispersion of which can be tuned as a function of the process duration..

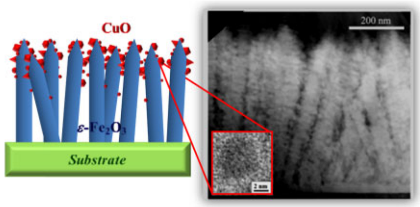

D. Barreca,* G. Carraro, D. Peeters, A. Gasparotto, C. Maccato, W. M. M. Kessels, V. Longo, F. Rossi, E. Bontempi, C. Sada, A. Devi

Chem. Vap. Deposition **2014**, *20*, 313 ... 319

Surface Decoration of ε-Fe_2O_3 Nanorods by CuO Via a Two-Step CVD/Sputtering Approach

Full Paper: ZrO_2 thin films are deposited by metal-organic (MO)CVD using the precursor $(Zr(NMe_2)_2(guan)_2)$ as the Zr source, together with oxygen. Functional properties, including the optical, electrical, and mechanical properties, of the resulting ZrO_2 films are investigated.

V.-S. Dang,* M. Banerjee, H. Zhu, N. B. Srinivasan, H. Parala, J. Pfetzing-Micklich, A. D. Wieck, A. Devi

Chem. Vap. Deposition **2014**, *20*, 320 ... 327

Investigation of Optical, Electrical, and Mechanical Properties of MOCVD-grown ZrO_2 Films